

## Quality assessment of urban trees: A comparative study of physiological characterisation, airborne imaging and on site fluorescence monitoring by the OJIP-test

Christian Hermans<sup>1,2,a</sup>, Mathias Smeyers<sup>3</sup>, Ronald Maldonado Rodriguez<sup>1</sup>, Murielle Eyletters<sup>2</sup>, Reto J. Strasser<sup>1</sup>, Jean-Paul Delhay<sup>2\*</sup>

<sup>1</sup> Bioenergetics Laboratory, University of Geneva, chemin des Embouchis, CH-1254, Jussy-Geneva, Switzerland

<sup>2</sup> Laboratoire d'Agrotechnologies Végétales – CP169, Université Libre de Bruxelles, 50 Av. F.D. Roosevelt, B-1050 Brussels, Belgium

<sup>3</sup> Laboratoire de Physiologie Végétale – CP206-2, Université Libre de Bruxelles, Campus Plaine, Bd. du Triomphe, B-1050 Brussels, Belgium

Received June 30, 2002 · Accepted August 3, 2002

### Summary

The purpose of this paper is to demonstrate the complementary utility of chlorophyll fast fluorescence OJIP transient (from 50 μs to 1 s) measurements in the aerial study of rows of trees. We identify limitations in photochemical events induced by urban injuries on *Platanus acerfolia* L., using the JIP-test procedure. The Performance Index (PI<sub>ABS</sub>) showed the largest dynamic range to characterise the vitality of trees. Individual trees were graded into three quality groups based on the individual PI<sub>ABS</sub> value compared to the overall average for trees in the alley. These groups are: high performers, with PI<sub>ABS</sub> 50 % higher than the alley average; normal trees, with a deviation from the alley average between –50 % and +50 %; and poor performers, whose deviation from the alley average was –50 % or less. Trees also were grouped into five vitality categories on the basis of a stereoscopic and morphologic observation of the symmetry of tree crowns, percentage of defoliation and reflectance property in the visible and infra-red range. Here, we report a remarkable correlation between the airborne remote sensing data and the on-site fluorescence measurements.

**Key words:** Chlorophyll fluorescence – Tree vitality – Urban stress factors – Performance Index

**Abbreviations:** ABS = absorption flux. – Chl *a* = chlorophyll *a*. – CS = cross section. – DF = driving force. – DIO = dissipation flux. – ETO = electron transport flux. – F<sub>M</sub> = maximal fluorescence level. – F<sub>O</sub> = F<sub>50μs</sub> = minimal fluorescence level. – F<sub>V</sub> = (F<sub>M</sub> – F<sub>O</sub>) = maximal variable fluorescence. – φ<sub>Po</sub> = F<sub>V</sub>/F<sub>M</sub> = yield of primary photochemistry. – I = intermediate step in the Chl *a* fluorescence transient at 2 ms. – J = intermediate step in the Chl *a* fluorescence transient at and 30 ms. – PI = performance index. – PSII = photosystem II. – Q<sub>A</sub> = primary quinone electron acceptor of PSII. – Q<sub>B</sub> = secondary quinone electron acceptor of PSII. – RC = reaction centre. – TRo = energy flux for trapping

\* E-mail corresponding author: [jpdelhay@ulb.ac.be](mailto:jpdelhay@ulb.ac.be)

<sup>a</sup> Present address: Laboratoire de Physiologie et de Génétique Moléculaire des Plantes, ULB-Plaine Bd du Triomphe CP 242, B-1050 Brussels, Belgium

## Introduction

Parks and gardens are a vital recreational element in our towns and cities. It has been recognised that these vegetative 'islands' provide more than an aesthetic contribution to the quality of life. Therefore, efforts have been made to emphasise the importance of trees in cities, and it has become a priority to investigate the behaviour and physiological needs of trees. Urban plants must tolerate hostile environmental conditions that affect plant health. Tree photosynthesis is restricted by the stress induced by various artificial environmental forces. These include nutrient deprivation (Pereira et al. 1992, Morales et al. 2000), drought (Marsal and Girona 1997), water excess and soil compaction (Day et al. 2000), and chemical soil pollution due mainly to the accumulation and storage of de-icing salts (Percival et al. 1998). Moreover, atmospheric pollutants such as ozone (Lütz et al. 2000, Clark et al. 2000a) combine with climatic stress factors such as limiting or excess solar radiation (Sullivan and Teramura 1994, Zeuthen et al. 1997) and wind speed (Clark et al. 2000b), to damage tree health. Given such conditions, the demand for diagnostic tools to measure tree vitality has become significant. Visual examination of leaf senescence and analytical procedures are used to assess tree vitality. Representative soil and leaf sampling, followed by analysis using standard or approved techniques, confirms the availability of mineral nutrients, but does not convey any accurate information about physiology. It has become common in most urban management projects to probe tree physiology by 'biosensing' techniques. Application of biospectroscopy to environmental investigation mainly involves spectral reflectance and chlorophyll fluorescence monitoring. Leaf pigment content can be determined *in situ* by spectral reflectance measurement (Gitelson and Merzlyak 1994, Peñuelas and Filella 1998, Barton 2001). By analysing the reflected light at a distance, it becomes possible to infer plant biomass and growth performance. Chlorophyll fluorescence techniques complete the investigation into the photosynthetic rates of plants under varied environmental conditions. Chlorophyll *a* fluorescence emitted by PSII turns out to be an easy tool for screening the photosynthetic vitality of plants as well as tissues and cells (Strasser et al. 1995). Accurate information on the efficiency of photochemical and de-excitation processes involved in light conversion can be gathered using this technique (Maxwell and Johnson 2000). As PSII is known to be one of the prime victims of stress conditions (Zeuthen et al. 1997, Morales et al. 2000), inferring PSII behaviour provides a diagnosis of the primary stress effects of urban injuries on the trees. Moreover, the technical possibilities in opto-electronics offer ways to infer biophysical aspects of samples *in situ*. The common approach of fluorimetric studies consists of measuring the fluorescence origin and maximum values, and in calculating parameters such as  $F_V/F_M$  ratio. Strasser et al. (2000) have provided a further analysis of the OIJP fast fluorescence rise, measured from 50  $\mu\text{s}$  to 1 s upon illumination of the

photosynthetic sample, and has discovered the bridge between this physical signal and the biological functions. Srivastava et al. (1999) developed a Performance Index that has permitted precise documentation of the vitality decrease of beech fumigated with  $\text{O}_3$  (Clark et al. 2000a).

For a global approach to stress detection, infra-red aerial images assist in evaluating weak trees for which support is required. The aim of this work is to demonstrate the complementary utility of fluorescence measurements for the study of urban tree vitality. We compare the stereoscopic analysis drawn from aerial pictures and correlated by field observation with parameters derived from the fast fluorescence rise. We show that study of the JIP-test parameters provide an overview of the effect of urban stress on trees.

## Material and Methods

### Location

The study was performed on August 29 and 30, 1999, on two rows of centenary *Platanus acerfolia* L., located on the Boulevard du Souverain in the city of Brussels, Auderghem. The avenue, oriented in a North-South direction, supports heavy traffic on 2x3 lanes. The trees are planted on a central parking platform, covered with compacted sand and raw dolomite.

### Chl *a* fluorescence transient measurements

To characterise their vitality, 40 fast fluorescence transients were recorded on leaves from the crowns of 60 trees. Measurements at ambient temperature were performed with a *Plant Efficiency Analyser* chlorophyll fluorometer (Hansatech Instruments, King's Lynn, Norfolk, UK). During the measurement, the sample was shielded from ambient light by a clip system to reach a dark adapted state (30 min adaptation to the dark) and illuminated with 660 nm light from an LED source built into the fluorometer sensor. Continuous light excitation (at 4500  $\mu\text{mol}/\text{m}^2\text{s}$ ) was provided by an array of six light-emitting diodes focused on the leaf surface to provide homogeneous irradiation over a 4 mm diameter leaf surface.

Fluorescence levels  $F_O$  (50  $\mu\text{s}$ ),  $F_{300\mu\text{s}}$ ,  $F_J$  (2 ms),  $F_I$  (30 ms) and  $F_M$  ( $tF_{\text{MAX}}$ ) were recorded. The *BioLyzer* software (Maldonado Rodriguez 2002) was used to load the full fluorescence transients and to calculate the JIP parameters from the variable fluorescence values at the times listed above, according to the equations of the JIP-test (Strasser and Tsimilli-Michael 2001).

### Aerial images acquisition

Photographs were taken on film (*Kodak Aerochrome Infrared Film 2443 – Estar Base*) with a spectral range from green to near infra-red. The pictures were analysed by Eurosense® based on a stereoscopic morphological observation, classifying trees into five vitality categories.

### Statistical treatment

The five points  $F_{50\mu\text{s}}$  ( $= F_O$ ),  $F_{300\mu\text{s}}$ ,  $F_{2\text{ms}}$ ,  $F_{30\text{ms}}$  and  $F_M$  extracted from the fluorescence transient were analysed. The difference of means

between the categories of trees was tested using a univariate analysis of variance test (ANOVA). The statistical analyses were done using the SAS system.

## Results

### Airborne remote sensing

Aerial images are regularly made by Eurosense®, a company specialising in airborne remote sensing and in picture interpretation. For the investigation presented here, one aerial picture of the *Boulevard du Souverain* is shown in Figure 1. Tree sanitary state is described in five classes, with respect to overall degree of damage. Each tree was placed within one of five categories numbered from 0 to 4. The vitality criteria of the five categories are defined as follows: Cat 0 – worst, nearly dead or totally defoliated trees. Cat 1 – partially defoliated trees, in unsatisfactory health conditions, with a category subdivision based on the crown characteristics (symmetrical, irregular and totally irregular crown). Cat 2 – trees showing an abnormal crown reflection in the visible range compared to the usual colours for the tree species in non stress conditions. A subdivision regroups trees according to the functionality of the decoloured portion of the crown on real colour images: less than 1/3, between 1/3 and 2/3, and more than 2/3. Cat 3 – trees without any external visual degradation symptoms, but which show a deviation in infrared reflection. Cat 4 – healthy trees whose health characteristics do not fit within categories 0 to 3. Moreover, concrete and direct information based on the stereoscopic interpretation of the picture are provided. The following management practices are proposed: cutting down, emergency aids, less urgent aid, and no action required. Typically, trees fitting with the category 1 are 2016 to 2022 (irregular leafy crown), with category 2: 2003, 2005, 2440 and 2442 (abnormal crown colours in visible range), with category 3: 2007 and 2009 (symmetrical crown, but showing abnormal reflection in the infrared), and with category 4: 2441 and 2409 to 2413 (symmetrical crown with intense colouration).

### On-site fluorescence measurements

In the alley, branches were cut from the crowns of sixty trees, labelled and kept in darkness for at least an hour before measuring. About 40 samples per tree were measured, each for one second, with a saturating red actinic light delivered by the portable fluorometer *PEA* (see Materials and Methods). 1200 digital data points per sample were analysed using the JIP-test procedure (Strasser et al. 1995, 2000).

The appendix shows the derivation of some biophysical characteristics (energy fluctuations and yields) calculated from the minimum and maximum fluorescence intensities ( $F_0$  and  $F_M$ ) and the fluorescence intensities selected at 300  $\mu$ s,



**Figure 1.** Airborne false colour image of the *Boulevard du Souverain* in Brussels, Belgium (altitude: 600m). Each tree in the alley is labelled by the indicated identity number. A quality assessment of 60 trees has been done on the image (see Materials and Methods) and by fluorescence measurements (JIP-test).

2  $\mu$ s and 30  $\mu$ s. A highly simplified working model of the energy fluctuations in the chloroplast is shown on Figure 2.

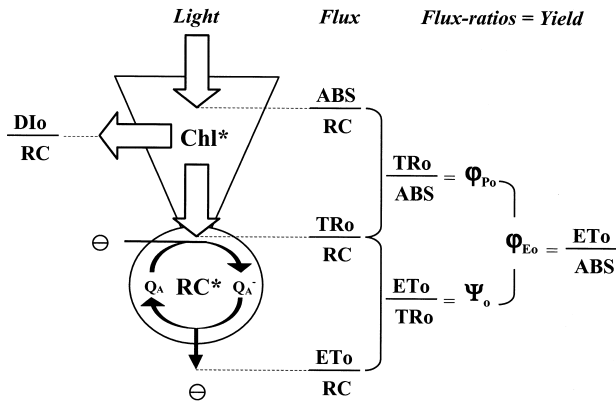


**Figure 2.** Energy cascade from solar light to photosynthetic electron transport in chloroplasts. ABS refers to the photon flux absorbed by the chlorophyll antenna pigments  $\text{Chl}^*$  of the photosystem II. Part of this excitation energy  $D_{Io}$  is dissipated, mainly as heat and less as fluorescence emission. Another part is channelled to the reaction centre RC, as trapping flux  $TR_o$ . In the reaction centre, the excitation energy is converted into redox energy by reducing the electron acceptor  $Q_A$  to  $Q_A^-$ , which is then reoxidised to  $Q_A$ , creating an electron transport  $ET_o$ . The three yields  $\phi_{P_o}$ ,  $\psi_o$  and  $\phi_{E_o}$  are directly related to the three energetic fluctuations, as the ratio of any two of them. The maximum quantum yield of primary photochemistry  $\phi_{P_o} = TR_o/ABS$  represents the probability that an absorbed photon is trapped by the RC and used for primary photochemistry, reducing  $Q_A$  to  $Q_A^-$ .  $\psi_o = ET_o/TR_o$  represents the efficiency with which a trapped exciton moves an electron further than  $Q_A^-$  in the electron transport chain.  $\phi_{E_o} (= ET_o/ABS)$  represents the probability that an absorbed photon moves an electron into the electron transport chain. Therefore  $\phi_{E_o} = \phi_{P_o} \cdot \psi_o$ .

An overall photosynthetic Performance Index (PI) has been defined and was calculated for each sample (Strasser et al. 2000). The overall PI of the alley is given by the average of all measured PIs (about 2400 samples). This value allows the grading of each individual tree into three quality groups, one above, one below and one within the average of all trees. The deviation of the average PI value of each tree from the reference value of the alley is indicated in Figure 3 as  $+\Delta PI_{ABS}$  respectively  $-\Delta PI_{ABS}$ . Two groups were selected from the 60 trees: one with the high performer trees with a  $\Delta PI_{ABS}$  value higher than +50% and the second group of poor performer trees with a  $\Delta PI_{ABS}$  value exceeding -50%. ANOVA statistical analyses on means of the 5 fluorescence values extracted from the OJIP transient [ $F_{50\mu s} (= F_o)$ ,  $F_{300\mu s}$ ,  $F_{2ms}$ ,  $F_{30ms}$  and  $F_M$ ], indicate significant differences ( $\alpha = 0.05$ ) among the 3 categories (high performer, normal and poor performer trees).

The relative Performance Index  $PI_{ABS}$  was compared to the electron transport (Fig. 4). All calculations are presented relative to the total chlorophyll absorption. The data for all trees fell on a straight line when the photosynthetic Driving Force ( $DF = \log PI$ ) was plotted against the relative electron transport activity ( $ET_o/ABS)_{rel}$ . The data in Figure 4 clearly show

that the selected trees fall on both extremes of the plot. All poor performer trees have low values, while high performer trees show the highest values. The axis of Figure 4 is chosen in such a way that the force/flux relationship becomes apparent in the straight line within the coordinate system driving force versus electron transport. The slope of this line ( $DF = \log PI$  within the coordinate system versus  $ET_o/ABS$ ) can be considered as a typical property of all measured trees in the transformation of absorbed light energy into chemical energy that is conducted further to the metabolic reactions. Figure 4 also allows comparison of the sensitivity of the two parameters  $DF_{rel}$  and  $ET_o/ABS$ . It appears that the most sensitive parameter calculated according to the equations of the JIP-test is the Performance Index. For example, for a deviation of 100% from the PI average value of trees, the electron transport would only increase of about 25%.

The main goal of this investigation is to determine whether or not a direct correlation exists between the airborne remote sensing data and the on-site fluorescence measurement. The variations in the PI values versus the quality classes from 0 to 4, defined on the basis of the airborne images, show an exponential relationship (Fig. 5A). By fitting the exponential curve to the data, a minimum PI value (called  $PI_{As}$ ), which corresponds to the asymptote of the function, can be determined. Therefore, the logarithmic value of the ratio  $PI_{rel} - PI_{As}$  falls on a straight line when plotted against the quality class from zero to five (Fig. 5B). The average PI value of all 60 trees falls between the quality class 2 and 3. According to the performance index, PI, the high performer trees fall into the quality class 4 and the poor performer trees into the quality class 1, on the scale established from aerial photographs.

Beside the Performance Index and electron transport (e.g. Fig. 4), the JIP-test allows calculation of different types of biophysical expressions such as vitality indices, phenomenological fluctuations, flux ratios or yields and specific fluctuations (see Appendix for calculations). To study the mechanisms of photosynthesis in each sample (e.g. for the high performer trees or poor performer trees in Fig. 6), so-called pipeline models have been developed and can be calculated and drawn on the basis of the experimental signals. For each group of trees, two pipeline models are shown. One is the membrane model, regrouping the specific energy fluctuations  $ABS/RC$ ,  $TR_o/RC$ ,  $D_{Io}/RC$  and  $ET_o/RC$  and the average antenna size per one active reaction centre (open small circle). The second model, the leaf model, shows the phenomenological energy fluctuations per leaf cross section, or leaf area, such as  $ABS/CS$ ,  $TR_o/CS$ ,  $D_{Io}/CS$  and  $ET_o/CS$  and the density of fully active reaction centres (open white circles). The small black circles are calculated as heat sinks that absorb the light in the same way as active reaction centres. These heat sinks are not able to store the excitation energy as redox energy, however, but they dissipate their total excitation energy as heat (heat sink centres or silent centres). The green colour of the sample or chlorophyll content per cross section is calculated by the Biolyzer software and drawn as the back-

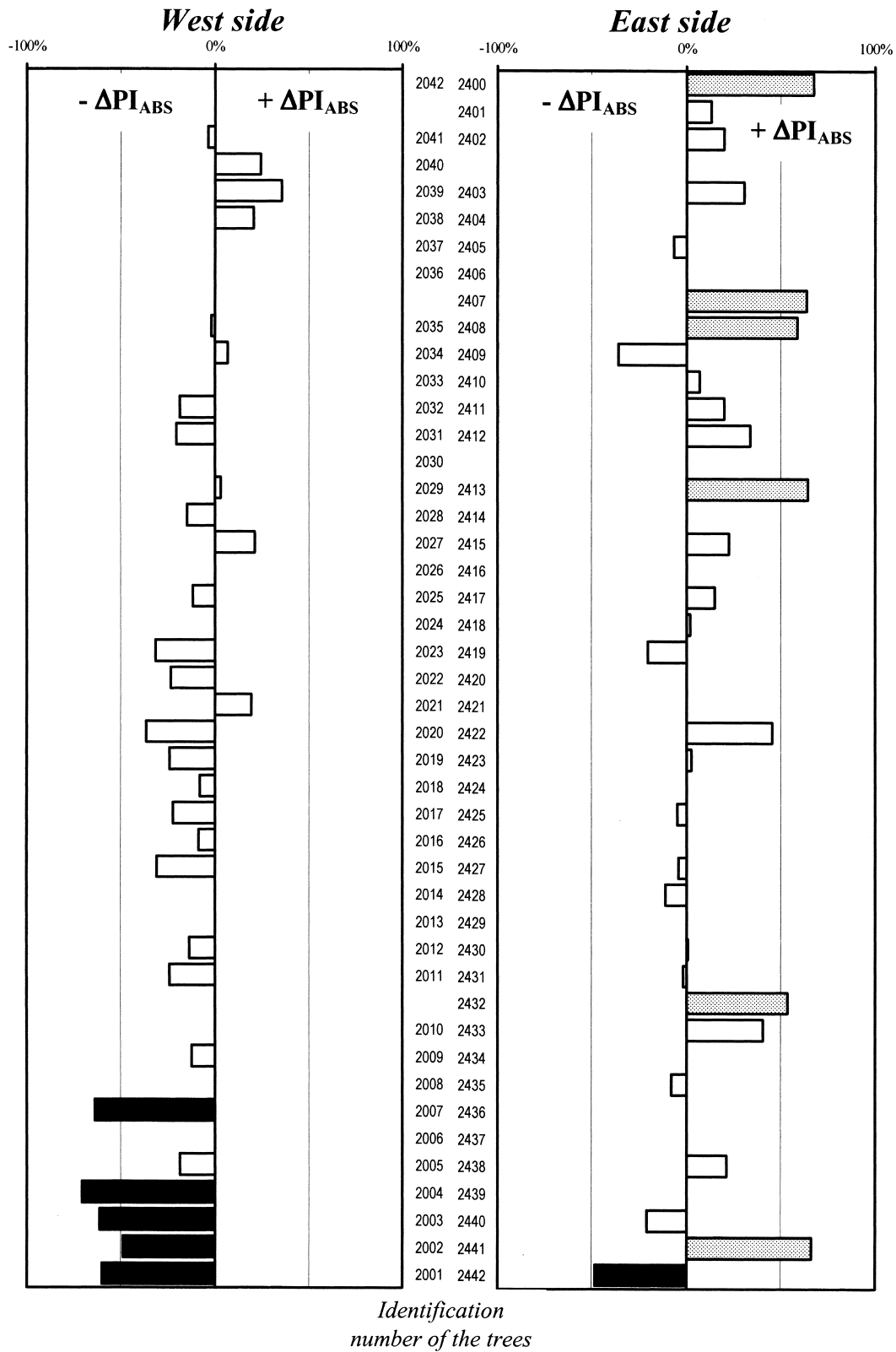


**Figure 3.** Relative deviation of the performance index  $PI_{ABS}$  of each tree from the average  $PI_{ABS}$  of all trees through the boulevard.  $\Delta(PI_{ABS})_{rel} \% = 100 \times [(PI_{ABS})_{tree} - (PI_{ABS})_{avg}] / (PI_{ABS})_{avg}$ . Black columns: poor performer trees with  $PI_{ABS}$  lower than 50% of  $(PI_{ABS})_{avg}$ , grey columns: high performer trees with  $PI_{ABS}$  50% higher than  $(PI_{ABS})_{avg}$  and white columns: trees within the tolerance  $(PI_{ABS})_{avg} \pm 50\%$ . The numbers identify the trees as shown on the aerial image on Figure 1.

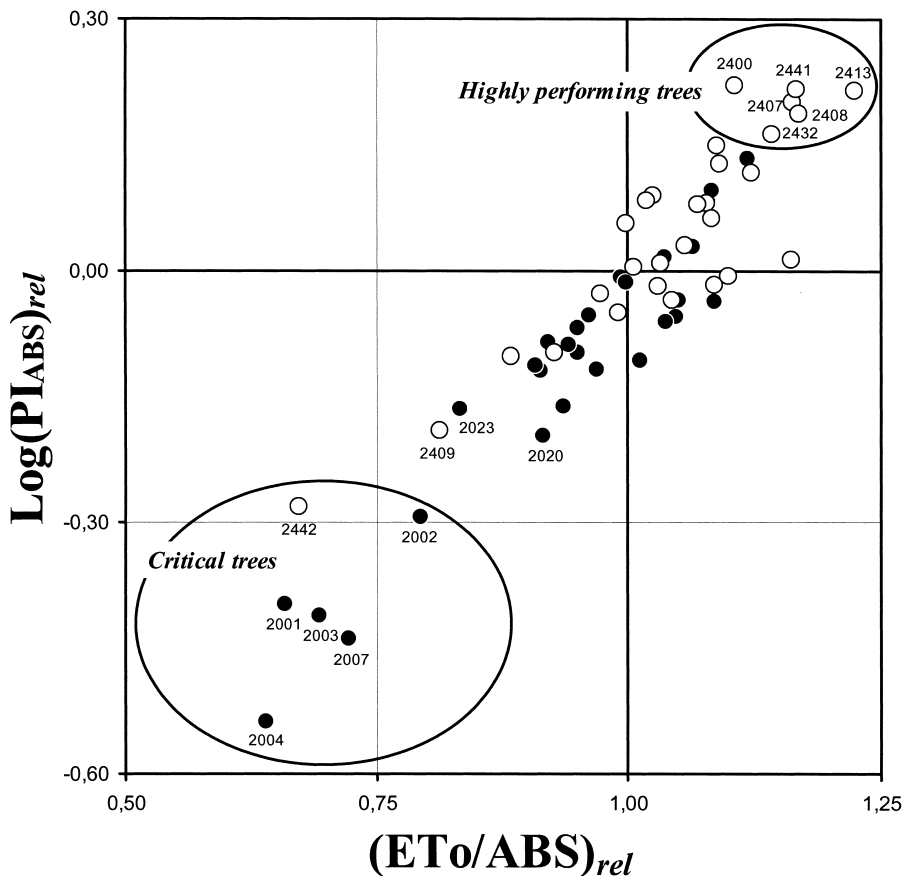


**Figure 4.** Correlation of the driving force  $\Delta(DF_{ABS})_{rel} = \text{Log}(PI_{ABS})_{rel}$  as a function of the relative yield of electron transport  $(ETo/ABS)_{rel} = [(ETo/ABS)_{tree} - (ETo/ABS)_{avg}] / (ETo/ABS)_{avg} = \text{Log}(PI_{ABS})_{rel} = \text{Log}[(PI_{ABS})_{tree} / (PI_{ABS})_{avg}] = \text{Log}(PI_{ABS})_{tree} - \text{Log}(PI_{ABS})_{avg} = \Delta(DF_{ABS})_{rel}$ . Filled circles West side and open circles East side. The six selected high performer trees and poor performer trees of Figure 3 are shown in the indicated areas. Note the linear relationship of the driving force versus the electron transfer (relative to the amount of chlorophyll).

ground grey colour of the leaf model. It appears that the poor performer trees have much less chlorophyll per cross section and fewer active units (open circles) than high performer trees. Therefore, the poor performer trees have a much lower electron transport per leaf cross section.

## Discussion

In the context of a biophysical approach toward assessing tree quality, fluorescence measurement techniques offer a way to measure fluorescence at canopy leaf scale. Different methods can be used to approach the leaves with the instrument. In the experiments reported in this work, tree climbers cut the branches.

Opto-electronic techniques explore biophysical aspects of photosynthetic functions close to the PSII of many trees. This powerful method allows the rapid and cost effective establishment of databanks containing large data sets. Moreover, the theoretical JIP-test concept (Strasser et al. 1995, 1996, Srivastava et al. 1999, Strasser and Tsimilli-Michael 2001), de-

rived from the primary fluorescence signal, is successfully applied to screen tree vitality in the particular biotope of the city. Among the constellation of the JIP expressions, one of the most sensitive is the PI. This parameter encompasses fluorescence transient changes associated with changes in antenna conformation and energy fluctuations. Therefore, the PI helps to estimate tree vitality with high resolution. Furthermore, it provides a way of establishing vitality categories and distinguishing trees with respect to their photosynthetic behaviour. In order to establish these categories, the average PI is regarded as a common reference to all individual values. This reference allows the calculation of a relative score that could not be considered an absolute performance of the tree (e.g. *Platanus* performance). For instance, forest trees could have a higher PI than urban trees, which are submitted to anthropomorphic activities. In this case, the average value of the alley should be lower than the average value of a forest.

This study helps to establish a grading of the trees in the alley and to adapt care and maintenance programmes and adjust treatment of the most fragile trees. In order to approach an absolute vitality value, different sites (urban trees,

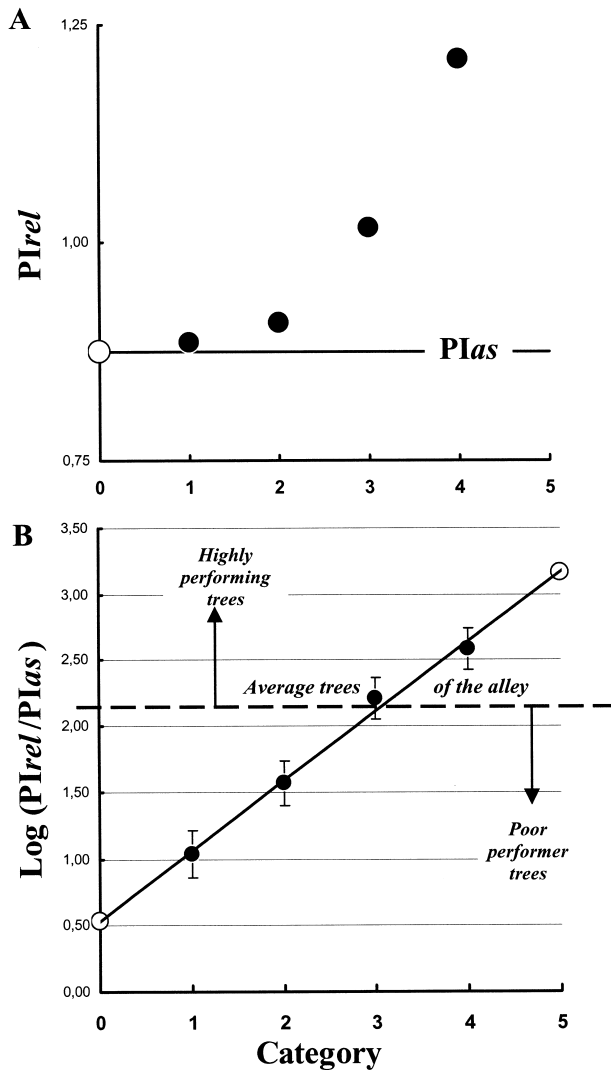


**Figure 5.** Comparison between the Performance Index and the stereoscopic morphological observations (category) based on the aerial image (see Fig. 1). Each tree has been classified in a category by an integer number ranging from one (worst, nearly dead tree) to four (most healthy tree). A. The average Performance Index ( $PI_{rel}$ ) of the trees and the score classification (category 1, 2, 3 and 4) are plotted on the ordinate. By exponential fitting, an asymptotic level  $PI_{as}$  was determined. B. A highly accurate ( $R^2 > 0.9$ ) linear relationship is shown between the  $\log(PI_{rel}/PI_{as})$  and the qualitative classification categories from zero to five. Filled circles: experimental values and open circles: calculated predictions.

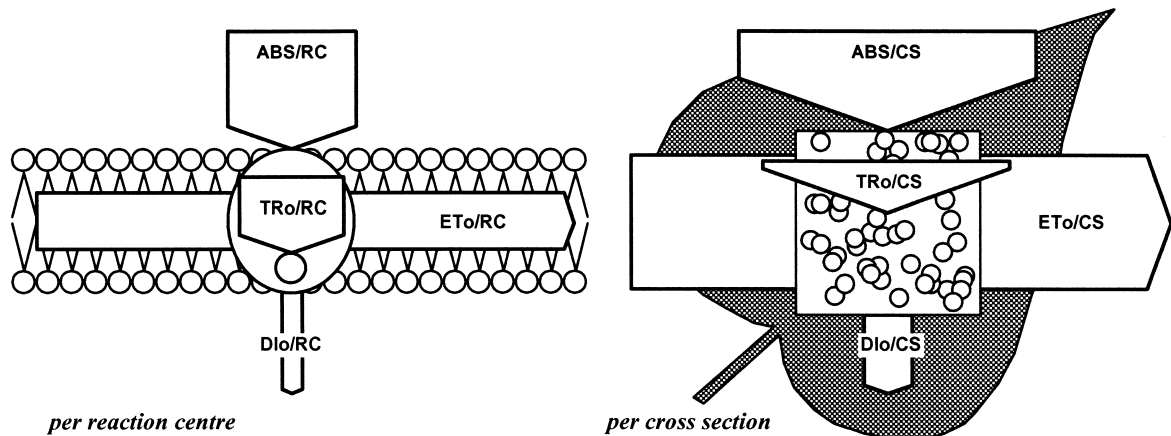
urban forests, urban green area and non urban forests) should be compared to infer species vitality. Comparison to other criteria may also serve as external references, for example on site morphological observations, other biophysical measurements (leaf reflectance, fluorescence imaging) or airborne image analysis. In this case, fluorometric investigation correlates remarkably well with stereoscopic morphologic observations and with the categories derived from it.

Quality mapping based on the individual Performance Index value is possible. This will create a sector map defining favourable and unfavourable zones and an individual map within each zone. The use of relative values also will enable comparison of the vitality of different tree species. Such mapping applied to the *Boulevard du Souverain* permits the detection of the most poorly performing trees situated to the South and the West of the alley. This will guide us in searching for the possible hostile factors present in that area. Finally, the pipeline model is a valuable tool for visualising the primary stages of photosynthesis. It gives a simple representation of the main energy fluctuations through the sample and it allows the visual comparison of various trees or groups of trees (e.g. poor performer versus high performer).

The reliability of the JIP-test, as well as the amount of information it provides, make it a sensitive tool for assessing the vitality of different biotopes. The limitation in the interpretation of the results comes from the fact that a number of stress factors are implicated. However, the method has been successfully applied in experimental conditions in which only one or a limited number of factors dominated (Clark et al. 2000 a, b, Tsimilli-Michael et al. 2000, Misra et al. 2001). It is clear that the trees within this alley present an extremely heterogeneous case. Therefore, traditional analytical approaches would be time consuming and expensive. The development of a biophysical test procedure as well as aerial remote sensing coupled with stereoscopic interpretation, provide a rapid method of measuring mean, including the possibility of characterising each tree as a distinct element in the alley. Although each of these techniques has advantages and disadvantages, they agree with each other and provide identical results. The aerial remote sensing method provides a quality assessment of a large city area, making it the most advantageous technique, but it requires highly qualified staff. By contrast, non specialised people can execute the fluorescence test at the leaf scale with commercial portable instruments and minimal instruction. Moreover, as the measuring time is very short (a few seconds per sample), the increased number of measured samples allows extensive statistical treatment of the data. The Performance Index, keeping a general overview of the photochemical events, correlates well with other, highly time-consuming quality assessment methods. Moreover, through the PI calculation, the heterogeneity of the vitality of trees in the alley could be described. The overall health of the alley has to be calibrated with other techniques and the estimations of specialists as well as by comparison with trees in similar situations. Each study contributes to the databanks concerning the health of urban trees and the accuracy of the quality assessment increases each time.

Finally, fluorometric investigation correlates remarkably well with classical tree observations. Its reliability and the amount of information derived provide an accurate and adequate tool for the vitality surveys of trees. The fluorescence technique is a tool used to distinguish normal and abnormal behaviour of the trees and it locates the problem in the special biotope of

### A. High performers



### B. Poor performers

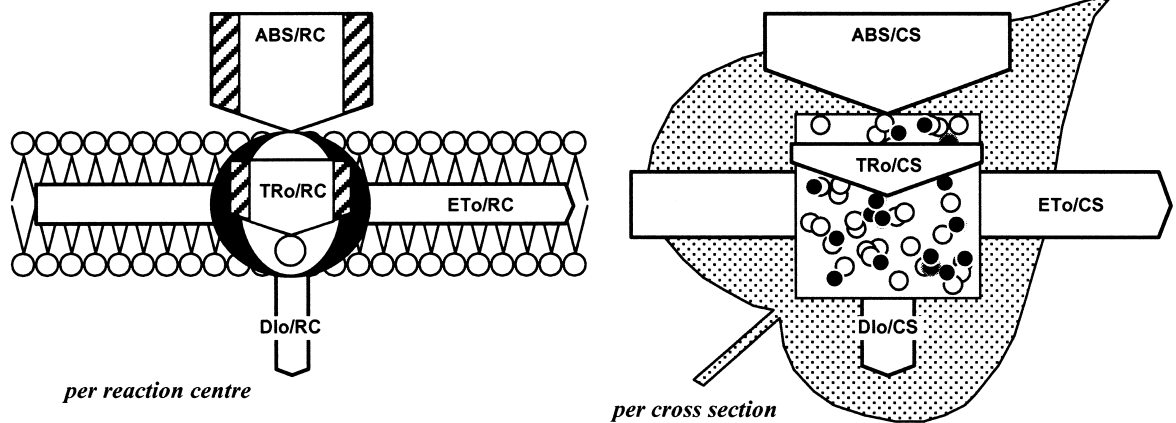


**Figure 6.** Energy pipeline models of the high performer (A) and poor performer (B) trees. The membrane models (left) represent the specific activities, expressed as fluctuation per reaction centre (RC). The leaf models (right) show the phenomenological fluctuations, expressed as per leaf cross section (CS). The relative magnitude of each activity or fluctuation is shown by the width of the corresponding arrow. The average antenna size is given as ABS/RC. This expresses the total absorption flux of PSII antenna chlorophyll divided by the number of active (in the sense of  $Q_A$  reducing) reaction centres. Thus, the antenna of PSII complexes with non- $Q_A$  reducing RCs (so called heat sink centres) are graphically added to the antenna of the active reactions centres. The absorption and trapping by PSII units with a heatsink centre is indicated as the hatched parts of the arrows ABS/RC and TRo/RC. The antenna belonging to the PSII units with heat sink centres is drawn in black while the antenna which belongs to the active ( $Q_A$  reducing) centres is drawn in white. In shaded zones of the leaf model, the  $Q_A$  reducing RCs per cross section are indicated by open circles and the non  $Q_A$  reducing RCs (heat sink or silent RCs) are indicated by the closed circles. The colouration of the foliage indicates the chlorophyll concentration per leaf cross section.

the city. The JIP-test procedure is a supplementary step in the quality assessment and allows an early diagnosis of most biological deregulation. It provides arguments for the politicians and helps to influence the decision for further phytosanitary intervention.

**Acknowledgements.** This study was commissioned and financed by the Ministère de la Région de Bruxelles-Capitale Administration de

l'Équipement et des Déplacements, Direction des Voiries (URL: arbres.irisnet.be), project supervisor Ir P. Basiaux. C. Hermans was supported by a grant from the Fonds pour la Formation de la Recherche dans l'Industrie et dans l'Agriculture, while he was at the Laboratoire d'Agrotechnologies Végétales. R. J. Strasser was supported by the project Interregio II (Urban Trees) and the Swiss National Foundation (Numerical Simulations). Aerial photography courtesy of the Ministère de la Région de Bruxelles-Capitale. Technical data on aerial photography are provided by Eurosense®. Special thanks to R. Mas-

saad from the Institut de Statistique et de Recherche Opérationnelle (Université Libre de Bruxelles, B) for the statistical support, and to Dr G. N. Johnson (Manchester University, UK) for proofreading.

## References

- Barton CVM (2001) A theoretical analysis of the influence of heterogeneity in chlorophyll distribution on leaf reflectance. *Tree Physiol* 21: 789–795
- Clark AJ, Landolt W, Bucher JB, Strasser RJ (2000a) Beech (*Fagus sylvatica*) response to ozone exposure assessed with a chlorophyll a fluorescence performance index. *Environ Pollut* 110: 1–7
- Clark AJ, Landolt W, Bucher JB, Strasser RJ (2000b) How wind affects the photosynthetic performance of trees: quantified with chlorophyll a fluorescence and open-top chambers. *Photosynthetica* 38(3): 349–360
- Day SD, Seiler JR, Persaud N (2000) A comparison of root growth dynamics of silver maple and flowering dogwood in compacted soil at differing soil water contents. *Tree Physiol* 20(4): 257–263
- Gitelson AA, Merzlyak MN (1994) Spectral reflectance changes associated with autumn senescence of *Aesculus hippocastanum* L. and *Acer platanoides* L. leaves. Spectral features and relation to chlorophyll estimation. *J Plant Physiol* 143: 286–292
- Lütz C, Anegg S, Gerant D, Alaoui-Sossé B, Gérard J, Dizengremel P (2000) Beech trees exposed to high CO<sub>2</sub> and to simulated summer ozone levels: Effects on photosynthesis, chloroplast components and leaf enzyme activity. *Physiol Plant* 109: 252–259
- Manoldo Rodriguez R (2002) <http://www.geocities.com/ResearchTriangle/Thinktank/8970/main1.html>
- Marsal J, Girona J (1997) Effects of water stress cycles on turgor maintenance processes in pear leaves (*Pyrus communis*). *Tree Physiol* 17: 327–333
- Maxwell K, Johnson GN (2000) Chlorophyll fluorescence – a practical guide. *J Exp Bot* 51(345): 659–668
- Misra AN, Srivastava A, Strasser RJ (2001) Utilisation of the fast chlorophyll a fluorescence technique in assessing the salt/ion sensitivity of mug bean and *Brassica* seedlings. *J Plant Phys* 158: 1173–1181
- Morales F, Belkhdja R, Abadía A, Abadía J (2000) Photosystem II efficiency and mechanisms of energy dissipation in iron-deficient, field-grown pear trees (*Pyrus communis* L.). *Photosynth Res* 63: 9–21
- Peñuelas J, Filella I (1998) Visible and near-infrared reflectance techniques for diagnosing plant physiological status. *Trends Plant Sci* 3(4): 151–156
- Percival GC, Biggs MP, Dixon GR (1998) The influence of sodium chloride and waterlogging stresses on *Alnus cordata*. *J Arboric* 24(1): 19–27
- Pereira JS, Chaves MM, Fonseca F, Araujo MC, Torres F (1992) Photosynthetic capacity of leaves of *Eucalyptus globulus* (Labill.) growing in the field with different nutrient and water supplies. *Tree Physiol* 11: 381–389
- Srivastava A, Strasser RJ, Govindjee (1999) Greening of peas: parallel measurements of 77 K emission spectra, OJIP chlorophyll a fluorescence transient, period four oscillation of the initial fluorescence level, delayed light emission, and P700. *Photosynthetica* 37(3): 365–392
- Strasser RJ, Srivastava A, Govindjee (1995) Polyphasic chlorophyll a fluorescence transient in plants and cyanobacteria. *Photochem Photobiol* 61: 32–42
- Strasser RJ, Eggenberg P, Strasser BJ (1996) How to work without stress but with fluorescence. *Bull roy Soc Liège* 65: 330–349
- Strasser RJ, Srivastava A, Tsimilli-Michael M (2000) The fluorescence transient as a tool to characterise and screen photosynthetic samples. In: Yunus M, Pathre U, Mohanty P (eds) *Probing Photosynthesis: Mechanisms, Regulation & Adaptation*. Taylor & Francis, London, UK, pp 445–483
- Strasser RJ, Tsimilli-Michael M (2001) Stress in plants, from daily rhythm to global changes, detected and quantified by the JIP-Test. *Chimie Nouvelle (SRC)* 75: 3321–3326
- Sullivan JH, Teramura AH (1994) The effects of UV-B radiation on loblolly pine.3. Interaction with CO<sub>2</sub> enhancement. *Plant Cell Environ* 17: 311–317
- Tsimilli-Michael M, Eggenberg P, Biro B, Köves-Pechy K, Vörös I, Strasser RJ (2000) Synergistic and antagonistic effects of arbuscular mycorrhizal fungi and *Azospirillum* and *Rhizobium* nitrogen-fixers on the photosynthetic activity of alfalfa, probed by the polyphasic chlorophyll a transient O-J-I-P. *Appl Soil Ecol* 15: 169–182
- Zeuthen J, Mikkelsen TN, Paludan-Müller G, Ro-Poulsen H (1997) Effects of increased UV-B radiation and elevated levels of tropospheric ozone on physiological processes in European beech (*Fagus sylvatica*). *Physiol Plant* 100: 281–290

**Appendix:** Derivation of the JIP-test parameters.

Technical parameters		
Fluorescence intensity at 50 $\mu$ s	$F_O$	
Maximal fluorescence intensity	$F_M$	
Variable fluorescence	$F_V$	= $F_M - F_O$
Slope at the origin of the normalised fluorescence rise	$M_O$	= $(F_{300\mu s} - F_O)/(F_M - F_O)$
Relative variable fluorescence at 2 ms	$V_J$	= $(F_{2ms} - F_O)/(F_M - F_O)$
Relative area between $F_M$ and $F_t$	$Sm$	= $F_O \int^{F_M} (F_M - F_t)/(F_M - F_O) dt$
The specific fluxes expressed per reaction centre (RC)		
Absorption per RC	$ABS/RC$	= $(M_O/V_J)/(1 - F_O/F_M)$
Trapping at time zero, per RC	$TRo/RC$	= $M_O/V_J = (ABS/RC) \phi_{P_o}$
Dissipation at time zero, per RC	$DIo/RC$	= $(ABS/RC) - (TRo/RC)$
Electron transport at time zero, per RC	$ETo/RC$	= $(TRo/RC) \Psi_O$
The phenomenological fluxes expressed per cross section of the leaf tissue (CS)		
Absorption per CS	$ABS/CS$	measured by absorption techniques or approximated by $F_O$ or $F_M$
Trapping at time zero, per CS	$TRo/CS$	= $(TRo/ABS)/(ABS/CS)$
Dissipation at time zero, per CS	$DIo/CS$	= $(ABS/CS) - (TRo/CS)$
Electron transport at time zero, per CS	$ETo/CS$	= $(ETo/RC)(RC/CS)$
Density of reaction centres per cross-section	$RC/CS$	= $(ABS/CS)(RC/ABS)$
The yields (or fluxes ratios)		
Maximum quantum yield of primary photochemistry	$\phi_{P_o}$	= $TRo/ABS = (F_M - F_O)/F_M$ = $1 - (F_O/F_M)$
Maximum quantum yield of non photochemical deexcitation	$\phi_{D_o}$	= $DIo/ABS = 1 - \phi_{P_o} = F_O/F_M$
Probability that a trapped exciton moves an electron further than $Q_A^-$	$\Psi_O$	= $ETo/TRo = 1 - V_J$
Probability that an absorbed photon moves an electron further than $Q_A^-$	$\phi_{E_o}$	= $\phi_{P_o} \Psi_O = (TRo/ABS)(ETo/TRo)$ = $ETo/ABS = (1 - F_O/F_M)(1 - V_J)$
Vitality Indexes		
Density of RCs per chlorophyll	$RC/ABS$	= $(RC/TRo)(TRo/ABS)$ = $(V_J/M_O)(F_V/F_M)$
Conformation term for primary photochemistry	$DF_{RC}$	= $\text{Log}(RC/ABS)$
	$[\phi_{P_o}/(1 - \phi_{P_o})]$	= $TRo/DIo = k_P/k_N = F_V/F_O$
	$DF_\phi$	= $\text{Log}[\phi_{P_o}/(1 - \phi_{P_o})]$
Conformation term for the thermal reactions (non light depending reaction beyond $Q_A^-$ )	$[\Psi_O/(1 - \Psi_O)]$	= $ETo/(dQ_A^-/dt_0)$
	$DF_\Psi$	= $\text{Log}[\Psi_O/(1 - \Psi_O)]$
Performance Index	$PI_{ABS}$	= $[RC/ABS][\phi_{P_o}/(1 - \phi_{P_o})][\Psi_O/(1 - \Psi_O)]$
Photosynthetic driving force of the sample on a chlorophyll basis	$DF_{ABS}$	= $\text{Log}[PI_{ABS}]$ = $DF_{RC} + DF_\phi + DF_\Psi$

## Note:

ABS is proportional to the concentration of antenna chlorophyll  $Chl_{ant}$ .

RC can also be written as reaction centre chlorophyll  $Chl_{RC}$ .

Therefore,  $RC/ABS = Chl_{RC}/Chl_{ant} = Chl_{RC}/(Chl_{tot} - Chl_{RC}) = (Chl_{RC}/Chl_{tot})/[1 - (Chl_{RC}/Chl_{tot})]$ .

The expression  $Chl_{RC}/Chl_{ant}$  is the probability that a chlorophyll molecule is a reaction centre chlorophyll. Therefore, the  $PI_{ABS}$  is composed of three expressions of the form  $P_x/(1 - P_x)$ . More components can be defined to make the PI a specific expression for many types of stress.